Metaheuristic Approach to Probabilistic Aircraft Conflict Detection and Resolution Considering Ensemble Prediction Systems

Eulalia Hernández-Romero, Alfonso Valenzuela, Damián Rivas, Daniel Delahaye

Metaheuristic Approach to Probabilistic Aircraft Conflict Detection and Resolution Considering Ensemble Prediction Systems

Eulalia Hernández-Romero*, Alfonso Valenzuela† and Damián Rivas‡
Department of Aerospace Engineering
Universidad de Sevilla
41092 Seville, Spain
Email:*ehernandez9, †avalenzuela, ‡drivas@us.es

Daniel Delahaye
Laboratoire de Mathématiques Appliquées Informatique et Automatique pour l'Aérien (MAIAA)
Ecole Nationale de l'Aviation Civile (ENAC)
F-31055 Toulouse, France
Email:delahaye@recherche.enac.fr

***Abstract*—This paper presents a methodology to tackle the problem of strategic aircraft conflict detection and resolution, up to 60 minutes in advance, considering wind and temperature uncertainties. The problem of hundreds of en-route aircraft flying multi-segmented 2D trajectories is considered. The weather uncertainty is retrieved from Ensemble Prediction Systems. The conflict detection is based on ensemble trajectory prediction, and is performed using an efficient grid-based procedure. A metaheuristic approach is developed to solve the conflicts, based on simulated annealing, which generates resolution trajectories by modifying the location of the route waypoints (vectoring), with the aim of lowering the probabilities of the conflicts while also minimising the deviation from the nominal paths. Realistic applications in scenarios with different traffic densities are presented.**

I. Introduction

The efficiency and safety of the Air Traffic Management (ATM) system is challenged by the ever increasing levels of air traffic demand. Projects around the world like SESAR in Europe, NextGen in the United States, and CARATS in Japan, work towards increasing the ATM system capacity and efficiency, while maintaining, or even improving, its safety levels. A promising approach towards meeting these goals is the development of automated decision support tools able to integrate and manage the uncertainty present in the ATM.

As discussed by Rivas and Vazquez [1], the ATM system is affected by several uncertainty sources, ranging from data uncertainty and unavailability to decisions taken by humans. Among these sources, weather uncertainty plays a key role in the ATM system performance: the limited knowledge about present and future meteorological conditions is responsible for many delays and flight cancellations, negatively affecting ATM efficiency and translating into extra costs for aircraft operators.

This paper addresses the problem of strategic aircraft conflict detection and resolution (CDR), up to one hour in advance, subject to weather uncertainty. In comparison to a tactical approach, strategic deconfliction enables the planning of more efficient resolution trajectories, while also reducing the workload of air traffic controllers [2]. Because the uncertainty in the prediction of the aircraft trajectories increases with extended time horizons, a probabilistic approach is necessary to tackle the strategic CDR problem.

The CDR problem has been widely studied in the literature, from both deterministic and probabilistic points of view. A review on CDR methods was presented by Kuchar and Yang in the year 2000 [3], and numerous studies on the subject have been published since then. More particularly, several examples of the integration of wind uncertainty into the CDR problem can be found in the literature. For instance, Matsuno et al. [4] present a stochastic methodology for mid-term conflict resolution, about 10 minutes in advance, considering a Gaussian spatially-correlated wind model; Rodionova et al. [5] develop several conflict resolution algorithms, at the strategic level of flight-planning, in the North Atlantic oceanic airspace.

In this paper, weather uncertainty data is retrieved from Ensemble Prediction Systems (EPS). Ensemble forecasts are found to represent weather uncertainties satisfactorily [6]. The use of EPS in trajectory prediction and CDR has been the subject of recent studies. Franco et al. [7] present a probabilistic trajectory predictor based on the Probabilistic Transformation Method (PTM) and apply it to the analysis of cruise flight time and fuel consumption considering wind uncertainties. Previous works by the authors [8,9] also apply the PTM method to the CDR problem for time horizons up to 20 minutes, a limited number of aircraft, and constant uncertain winds. Courchelle et al. [10] address the problem of strategic conflict resolution (CR), prior to take-off, using a worst-case approach to integrate wind and temperature uncertainties.

The methodology presented in this paper considers a time horizon of 60 minutes. It aims to expand the capabilities of conflict detection (CD) tools currently in use in Europe, such as Short-Term Conflict Alert (STCA) and Medium-Term Conflict Detection (MTCD), with time horizons of 2 and 20 minutes, respectively. Because aircraft travel hundreds of kilometres in one hour, the methodology is applied to a large airspace, as for example those handled by Area Control Centres, where hundreds of aircraft are simultaneously present.

Centralized conflict resolution is a highly combinatorial problem whose complexity significantly increases as the number of aircraft grows. Given the large number of aircraft considered in this work, a metaheuristic approach is convenient to tackle this problem. Metaheuristic approaches have already been used in large-scale CR problems by some authors: for example, Chaimatanan [11] uses a hybrid-metaheuristic approach based on Simulated Annealing (SA) to compute conflict-free trajectories on a continental scale; Courchelle et al. [10] also employ SA in strategic aircraft deconfliction covering a national airspace. The work presented in this paper follows these two works.

This paper focuses on the CDR problem of aircraft flying en-route multi-segmented 2D trajectories subject to wind and temperature uncertainties. The approach proposed in this paper can be summarized as follows. The wind and temperature uncertainties are retrieved from EPS; in particular, the European COSMO-D2-EPS is used. The CD methodology is based on ensemble trajectory prediction, where the aircraft trajectories are computed for each member of the ensemble to obtain an ensemble of trajectories. In comparison to a worst-case approach, this probabilistic methodology allows the computation of a probability of conflict by taking into account the contribution of each member of the ensemble. The conflict detection is performed using an efficient grid-based approach. The CR methodology uses the Simulated Annealing algorithm to generate resolution trajectories by modifying the trajectories' waypoints (vectoring). The objective is to lower the total probability of conflict between pairs of aircraft while minimising the deviation from the nominal paths.

This paper is structured as follows. First, EPS and their use in trajectory prediction are described in Section II. In Section III, the probabilistic trajectory prediction is presented. The conflict detection strategy is detailed in Section IV, followed in Section V by the description of the conflict resolution methodology. Results are presented in Section VI for two different conflict scenarios with low and high traffic densities. Finally, the conclusions and future steps of this work are discussed in Section VII.

II. Ensemble Prediction Systems

In order to characterise and quantify the uncertainty in a weather forecast, it is convenient to use a probabilistic approach. One of today's most promising trends in probabilistic forecasting is Ensemble Prediction Systems. An ensemble forecast comprises multiple runs of a Numerical Weather Prediction (NWP) model which differ in the initial conditions and/or the physical parametrisation of the atmosphere; some ensembles use more than one NWP model [12]. The goal is to generate a sample of possible future states of the atmosphere. The uncertainty information is on the spread of the members in the ensemble, and the hope is that this spread brackets the true weather outcome.

There are two main approaches for trajectory prediction subject to uncertainty provided by ensemble weather forecasts:

1) Ensemble approach: a deterministic trajectory predictor is used for each member of the ensemble, leading to an ensemble of trajectories from which probability distributions can be derived.
2) Transformation approach: probability distributions of meteorological parameters of interest (such as wind) are obtained from the ensemble forecast and evolved using a probabilistic trajectory predictor.

Previous works by the authors on probabilistic CDR followed the second approach [8,9]; a probabilistic trajectory predictor based on the Probabilistic Transformation Method was developed, limited to constant wind scenarios. In this paper, since the aircraft travel large distances and the atmospheric variables are expected to change, a deterministic trajectory predictor able to handle these changes is developed, and the ensemble trajectory prediction approach is followed.

In this work, the weather uncertainty is retrieved from COSMO-D2-EPS, developed and operated by the German Weather Service [13,14]. It is a 20-member ensemble which covers a wide area in central Europe, see Figure 1. This forecast is operated for the very short-range, has a fine-scale horizontal resolution of 2.2 km, and vertical resolution of 65 atmosphere levels. It is run at 00, 03, 06, 09, 12, 15, 18 and 21 UTC, providing hourly forecasts up to 27 hours. They are available about one hour after the run.

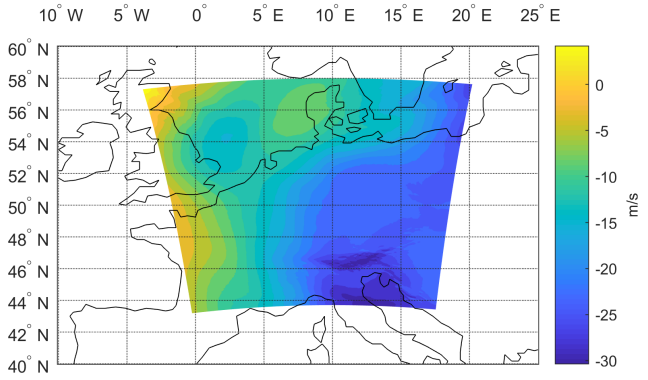

Figure 1. COSMO-D2-EPS: average meridional wind at pressure level 200 hPa. 3-hour forecast ran at 09 UTC 2019-02-14.

III. Ensemble Trajectory Prediction

Let us consider N aircraft flying in the same airspace and altitude, h. The aircraft follow multi-segmented 2D trajectories defined by a series of waypoints, provided by their flight plans. The aircraft trajectories are composed of straight segments and fly-by turns, as depicted in Figure 2.

The following assumptions are taken into consideration:

- An spherical, non-rotating Earth model is considered, with radius R_E.
- The aircraft motion is considered as that of a point mass with three degrees of freedom.
- The aircraft initial positions are certain and known.
- Each aircraft i flies at constant Mach number M_i, which is certain and known.

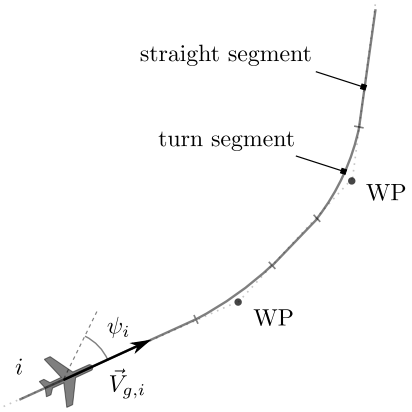

Figure 2. General trajectory for aircraft i.

- The aircraft are affected by horizontal uncertain winds, described by their zonal (West-East), w_λ, and meridional (South-North), w_φ, components. The air temperature, Θ, is also uncertain.
- Turns are modelled as constant radius turns. The turn radius R_i for each aircraft is that resulting from a constant bank angle, constant temperature given by the International Standard Atmosphere (ISA) at the aircraft's altitude, and no winds:

$$R_i = \frac{\left(M_i \sqrt{\gamma_g R_g \Theta_{ISA}(h)}\right)^2}{g \tan \mu}, \tag{1}$$

  where γ_g and R_g are the ratio of specific heats and the gas constant, respectively, $\Theta_{ISA}(h)$ is the air temperature given by the ISA model at altitude h, g is the gravitational acceleration, and μ is the bank angle.
- No turns are performed at the origin and destination waypoints of the trajectories.
- A quasi-steady state is assumed, thus the temporal and spatial derivatives of wind and temperature are negligible.

By considering the previous assumptions, the equations that describe the movement of aircraft i can be expressed as the following system of differential equations:

$$\frac{d\varphi_i}{dt} = \frac{1}{R_E + h} V_{g,i} \cos \psi_i, \tag{2}$$

$$\cos \varphi_i \frac{d\lambda_i}{dt} = \frac{1}{R_E + h} V_{g,i} \sin \psi_i, \tag{3}$$

$$\frac{dr_i}{dt} = \frac{R_E}{R_E + h} V_{g,i}, \tag{4}$$

$$\frac{d\psi_i}{dt} = \frac{1}{R_i} \frac{dr_i}{dt}, \tag{5}$$

being λ_i and φ_i the aircraft longitude and latitude, ψ_i the aircraft course, r_i the ground distance along the trajectory and $V_{g,i}$ the groundspeed. The straight segments of the trajectories are computed using Eqs. (2) to (4), with constant course, ψ_i; on the other hand, turn segments are computed using Eqs. (2) to (5), considering constant turn radius, R_i. The groundspeed of aircraft i is computed from its airspeed V_i using the velocity triangle, depicted in Figure 3, as follows:

$$V_{g,i} = \sqrt{V_i^2 - w_{XT,i}^2} + w_{AT,i}. \tag{6}$$

In this equation, $w_{XT,i}$ and $w_{AT,i}$ are the cross-track and along-track components of the wind affecting the aircraft, respectively, which can be obtained from the zonal and meridional wind components given by the weather forecast:

$$w_{XT,i} = w_\lambda \cos \psi_i - w_\varphi \sin \psi_i, \tag{7}$$

$$w_{AT,i} = w_\lambda \sin \psi_i + w_\varphi \cos \psi_i. \tag{8}$$

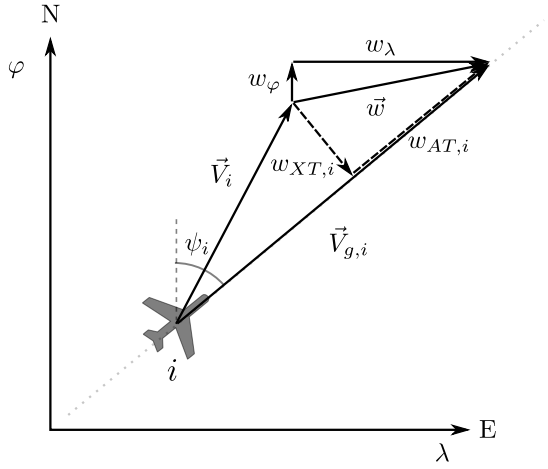

Figure 3. Velocity triangle for aircraft i.

The aircraft airspeed can be computed from its Mach number and the temperature given by the weather forecast as:

$$V_i = M_i \sqrt{\gamma_g R_g \Theta}. \tag{9}$$

The wind and temperature values for a particular location and time are linearly interpolated from the data provided by the EPS. Because the wind components and the air temperature are uncertain, the aircraft groundspeeds are also uncertain, and so are their positions along the trajectory at a given time.

The differential equations are integrated for each one of the 20 members of the EPS, resulting in an ensemble of 20 different trajectories for each aircraft. Figure 4 illustrates the computed advance or delay of each trajectory with respect to the mean flight time as a function of the travelled distance for one of the aircraft later used in the application. It can be clearly seen how the uncertainty increases for distant points.

IV. Conflict detection

A conflict between two aircraft exists when their future positions are predicted to be closer than a given set of separation minima. In a two-dimensional environment, as considered in this work, a conflict exists when the minimum horizontal distance between two aircraft is less than a minimum separation requirement D.

Since an ensemble of trajectories is predicted for each aircraft, the existence of a conflict is uncertain. The probability of conflict between aircraft i and j is obtained as follows:

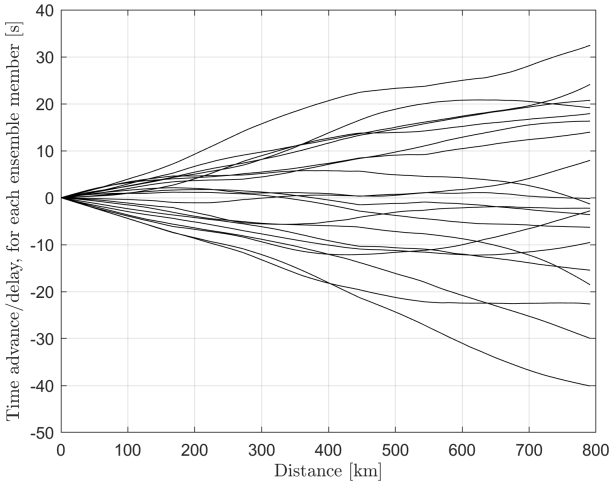

Figure 4. Advance or delay for each member of the ensemble of trajectories.

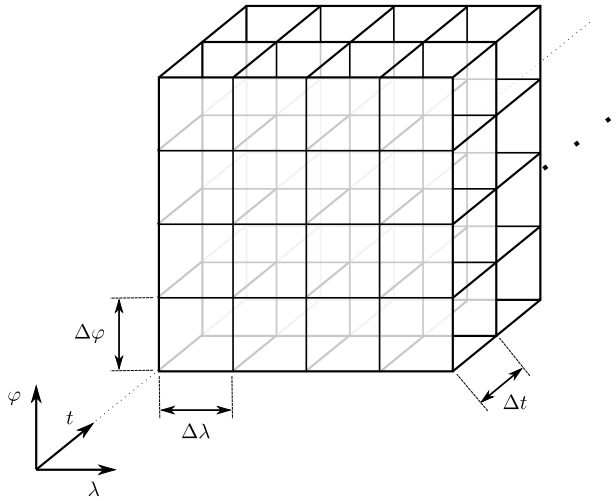

Figure 5. Three-dimensional (space and time) grids for each member of the ensemble.

1) For each member of the ensemble, m, the minimum distance between i and j, $d_{ij,m}$, is determined.
2) A conflict in member m between i and j, $c_{ij,m}$, is identified if the minimum distance is less or equal to the minimum separation requirement:

$$c_{ij,m} = \begin{cases} 1 & \text{if} \quad d_{ij,m} \leq D, \\ 0 & \text{if} \quad d_{ij,m} > D. \end{cases} \tag{10}$$

3) The probability of conflict between i and j, $P_{con,ij}$, is computed as the fraction of members for which a conflict is identified:

$$P_{con,ij} = \frac{1}{20} \sum_{m=1}^{20} c_{ij,m}. \tag{11}$$

The probability of conflict is pairwise determined for the N aircraft. In order to alleviate the computational effort of determining the minimum distance for all the aircraft pairs, which is very demanding for a high number of aircraft, a grid-based conflict detection scheme is used. This method, introduced by Jardin [15], aims at reducing the computational cost of the conflict detection problem at the expense of additional required computer memory.

The application of this method to the probabilistic conflict detection presented in this paper is as follows. For each one of the 20 members of the ensemble, a three-dimensional grid (longitude, latitude, and time) is constructed, as illustrated in Figure 5. The size of the cells in the spatial dimensions must be greater or equal to the minimum separation requirement, and the size in the temporal dimension should be small enough so no conflict goes unidentified. In each cell of the grid, a list of the aircraft occupying the cell is stored. In order to reduce the memory requirement, this information is stored as a hash table (see Hastings et al. [16]). Then, for aircraft i and j, if their trajectories occupy the same or adjacent cells, the minimum distance between the aircraft is calculated, and the conflict is characterized using Eq. (10); otherwise, the variable $c_{ij,m}$ is directly set to zero.

V. Conflict resolution

In this work, vectoring is chosen as the resolution manoeuvre, that is, conflicts are solved by modifying the trajectories' waypoints. Conflict resolution is formulated as an optimization problem where the objective is to lower the probabilities of the conflicts between pairs of aircraft while also minimising the deviation from the nominal paths. This problem is solved using the Simulated Annealing algorithm. Next, the decision variables, constraints, cost function, and the optimisation algorithm are described.

A. Decision variables

All the waypoints that define the flight path, with the exception of the initial points where the aircraft are located, are considered as modifiable. Thus, the decision variables are the coordinates of the modifiable waypoints.

For aircraft i, the decision variables are collected in a control matrix $\mathbf{u}_i$. Each row of this matrix, $\mathbf{u}_{ik}$, corresponds to one waypoint, the first element is the longitude of the waypoint, and the second element is the latitude:

$$\mathbf{u}_{ik} = [u_{ik_\lambda}, u_{ik_\varphi}], \qquad k = 1, \ldots, K_i, \tag{12}$$

where K_i is the total number of modifiable waypoints for aircraft i. An example is illustrated in Figure 6. In this Figure, the nominal path of the aircraft, collected in the matrix $\mathbf{u}_{0,i}$, is also depicted. The decision variables of the N aircraft are stored in a control set as follows:

$$\mathbf{u} = \{\mathbf{u}_1, \mathbf{u}_2, \ldots, \mathbf{u}_i, \ldots, \mathbf{u}_N\}, \qquad i = 1, \ldots, N. \tag{13}$$

B. Constraints

The decision variables are subject to the following two kinds of constraints:

1) The distance between consecutive waypoints k and $k+1$, L_{ik}, must be large enough to accommodate the fly-by turns performed at the each waypoint, see Figure 7. The

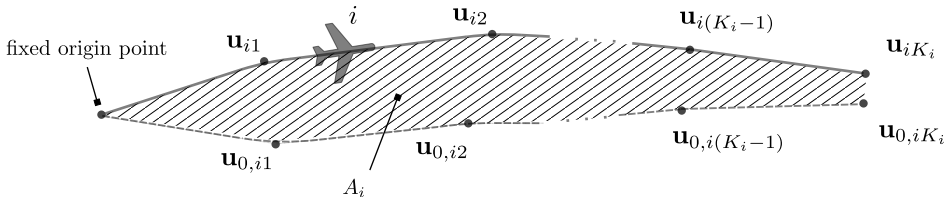

Figure 6. Decision variables for aircraft i.

minimum distance criterium recommended by ICAO for the design of flight procedures is considered [17]:

$$L_{ik} \geq l_{ik} + l_{ik+1}, \tag{14}$$

$$l_{ik} = R_i \tan(\alpha_{ik}/2) + 5V_i, \tag{15}$$

where l_{ik} is the minimum stabilization distance at waypoint k, and α_{ik} is the course change at waypoint k. Notice that the minimum stabilization distance considers a five second delay to take into account the bank establishing time. Since no turns are performed at the origin and destination waypoints, at these points the minimum stabilization distances are nil.

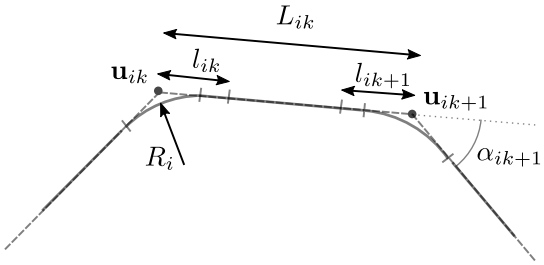

Figure 7. Minimum distance between waypoints.

2) To prevent large lateral deviations, the possible locations of the modified waypoints $\mathbf{u}_{ik}$ are bounded:

$$u_{ik_\lambda} \in [u_{0,ik_\lambda} - \delta\lambda/2, u_{0,ik_\lambda} + \delta\lambda/2], \tag{16}$$

$$u_{ik_\varphi} \in [u_{0,ik_\varphi} - \delta\varphi/2, u_{0,ik_\varphi} + \delta\varphi/2]. \tag{17}$$

where $\delta\lambda$ and $\delta\varphi$ are configurable limits. Figure 8 graphically illustrates this constraint.

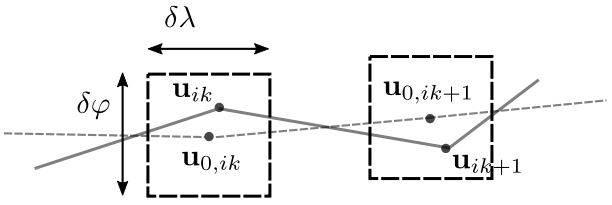

Figure 8. Decision variables boundaries.

C. Cost function

As previously stated, the objective is to minimise the probabilities of conflict between pairs of aircraft while minimising the deviation from the nominal paths. Taking this into account, the following cost function Φ is used:

$$\Phi = \sum_{i=1}^{N} \Phi_i = \sum_{i=1}^{N} \left(\sum_{j=1, j\neq i}^{N} (C_{ij} - \delta_{ij}) + a\frac{A_i}{L_{0,i}} \right). \tag{18}$$

where Φ_i is the cost related to trajectory i.

The variable C_{ij} represents the conflict probability between aircraft i and j; it is defined as:

$$C_{ij} = \begin{cases} P_{con,ij} & \text{if } P_{con,ij} \geq P_\tau \\ 0 & \text{if } P_{con,ij} < P_\tau \end{cases}, \tag{19}$$

where P_τ is a configurable probability threshold. This threshold differentiates between high- and low-probability conflicts; it aims to focus the resolution on certain conflicts and avoid wasting resources on conflicts which may not materialise.

Since the presented methodology is envisioned for strategic resolution, those aircraft that at the time of the prediction are in loss of separation should be solved by tactical tools, and are disregarded from this process. The variable δ_{ij} addresses this idea by removing the cost of these losses of separation from the cost function: it takes value one if aircraft i and j are in loss of separation at their initial positions and zero otherwise.

Finally, A_i is the area between the modified and the nominal path of aircraft i (defined by $\mathbf{u}_i$ and $\mathbf{u}_{0,i}$), as depicted in Figure 6, and $L_{0,i}$ is the total flight distance of the nominal trajectory. The ratio $A_i/L_{0,i}$ is an evaluation of the average lateral deviation from the original intent. The coefficient a is a configurable parameter used to balance the resolution of conflicts and the deviations from the nominal paths; this coefficient should be small enough so that this last term does not overpower the other two.

D. Simulated Annealing

In this work, hundreds of aircraft are simultaneously handled, deriving into thousands of decisions variables. Due to this complexity, the Simulated Annealing (SA) algorithm is chosen to solve the optimization problem. This metaheuristic technique was introduced in 1983 by Kirkpatrick et al. [18], inspired by the annealing process in metallurgy. In SA, the cost function is analogous to the energy of the physical process, and the decision variables are analogous to the coordinates of the material's particles. Next, the adaptation of the SA algorithm to the problem presented in this paper is described. The algorithm is summarized in the diagram in Figure 9.

1) Neighbourhood function: Starting from a current solution, described by the current state $\mathbf{u}_c$ (that is, the control set for the N aircraft) and cost Φ_c, the neighbourhood function generates a candidate solution by performing local modifications, creating a neighbour state $\mathbf{u}_n$ and a neighbour cost Φ_n. In the iteration, the current solution is described by the initial state (nominal paths) $\mathbf{u}_0$ and cost Φ_0. The neighbourhood function used in this work follows these steps:

1) First, an aircraft $i \in \{1, \ldots, N\}$ is randomly selected with a probability proportional to its individual cost Φ_i, therefore those aircraft that contribute the most to the cost function are more likely to be selected.
2) For the chosen aircraft i, a point $\mathbf{u}_{ik}$ is chosen by randomly selecting an index $k \in \{1, \ldots, K_i\}$.
3) The coordinates of $\mathbf{u}_{ik}$ are randomly modified inside the boundaries defined by Eqs. (16,17), following uniform statistical distributions. If the resulting coordinates do not comply with the constraint defined by Eq. (14), another index k is randomly selected and new coordinates are generated. This search is repeated until a new location for a point $\mathbf{u}_{ik}$ is accepted. This step guarantees that the neighbourhood state is feasible.

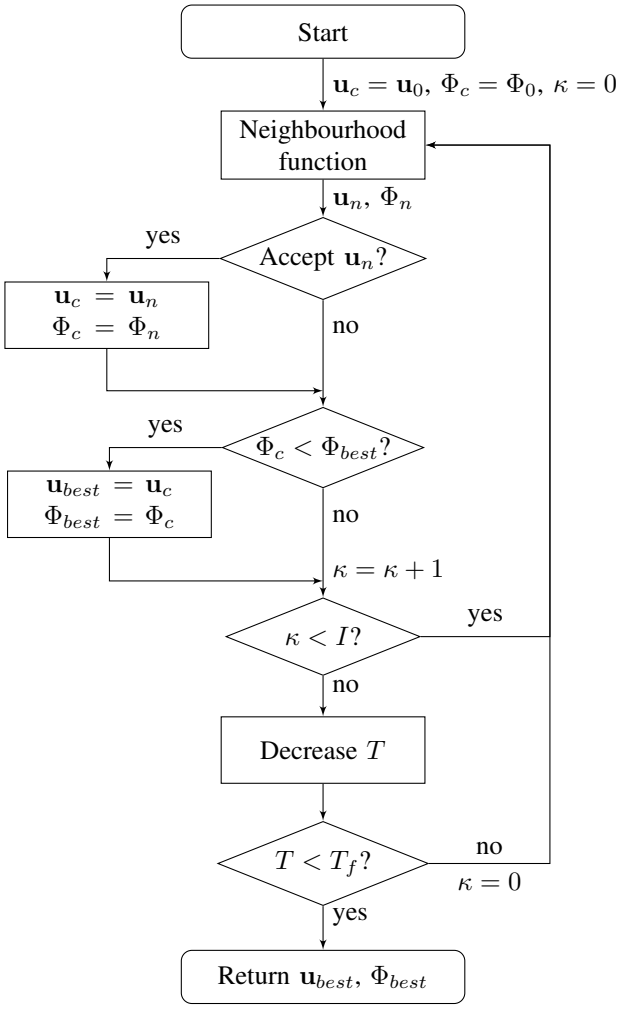

Figure 9. Simulated Annealing algorithm flow diagram.

2) Acceptance function: The acceptance function determines whether a neighbour solution is accepted or not. In this work, if the cost is improved ($\Phi_n < \Phi_c$), the solution is always accepted. Otherwise, there is a probability of accepting the solution that follows a Boltzmann distribution:

$$P_{accept} = e^{-(\Phi_n - \Phi_c)/T}, \tag{20}$$

where T is a varying parameter called *temperature*. The probability of acceptance decreases as the temperature decreases. If the neighbour solution is accepted, the current state and cost are updated to the neighbour state and cost.

3) Initial temperature: In this work, the initial temperature is chosen so that the initial acceptance rate is over a configurable threshold τ_0. The acceptance rate is computed by generating I neighbour solutions and evaluating the acceptance function in these solutions.

4) Cooling schedule: In this work, the temperature decreases following a geometrical law $T_c = \beta T_{c-1}$, where β is a configurable constant value between 0 and 1. A slow-decreasing temperature is more likely to produce a better solution than a fast-decreasing temperature, but it will require more computation time.

5) Equilibrium state: The equilibrium state is reached after a selected number of iterations I are performed at each temperature state.

6) Termination criterion: The algorithm stops and returns the final solution, $\mathbf{u}_{best}$ and Φ_{best}, when the temperature reaches a sufficiently small value so that the probability of acceptance becomes negligible. In this work, the process terminates when the temperature reaches a final value $T_f = \gamma T_0$, where γ is a configurable constant between 0 and 1.

VI. Application

Next, results are presented for two different scenarios: low and high traffic density. In both scenarios, the CDR process is launched at 12:00 UTC on the 14th of February of 2019, and conflicts are detected and solved for the next 60 minutes. The weather data is retrieved from COSMO-D2-EPS: in particular, the most recent available forecast, run at 09:00 with lead times of 3 and 4 hours, is used (since the weather forecasts are available about an hour after they are run, 12:00 forecast would not be yet available). The air traffic over Europe inside the EPS coverage area is considered. The flight data are collected from the last filed flight plans stored in Eurocontrol's Demand Data Repository (DDR). The aircraft Mach number and bank angle values are obtained from Eurocontrol's Base of Aircraft Data (BADA 3.13). In the first scenario, flights in the en-route phase at flight level FL380 at 12:00 are considered, resulting in an scenario with $N = 92$ aircraft. Those aircraft that at the starting time are not present in that flight level or in the designated area are not considered. The second, high-traffic-density, scenario is artificially generated by merging in a single level (FL380) all flights that are en-route in flights levels 370, 380, and 390 at 12:00, resulting in a total number of $N = 214$ aircraft. Notice that face-to-face severe encounters are found in this artificial and more demanding scenario.

The minimum separation requirement is $D = 5$ NM. The 3D-grid cells used in the conflict detection have a size of $\Delta\lambda = \Delta\varphi = 0.1^\circ$ and $\Delta t = 10$ s. The conflict resolution uses the following parameters: $\delta\lambda = \delta\varphi = 0.7^\circ$, $P_\tau = 50\%$, $a = 10^{-4}$ m^{-1}, $I = 200$, $\tau_0 = 50\%$, $\beta = 0.98$, and $\gamma = 10^{-5}$.

As an example of the effects of the methodology on the aircraft trajectories, Figure 10 shows the distance between two aircraft over time, for each member of the ensemble, before and after the conflict resolution. The dash-dotted line at 5 NM represents the minimum separation requirement. Before CR, for some members of the ensemble a conflict is detected at about 14 minutes, leading to a probability of conflict of 80%. After CR, and by modifying the trajectories, the conflict is solved for all members.

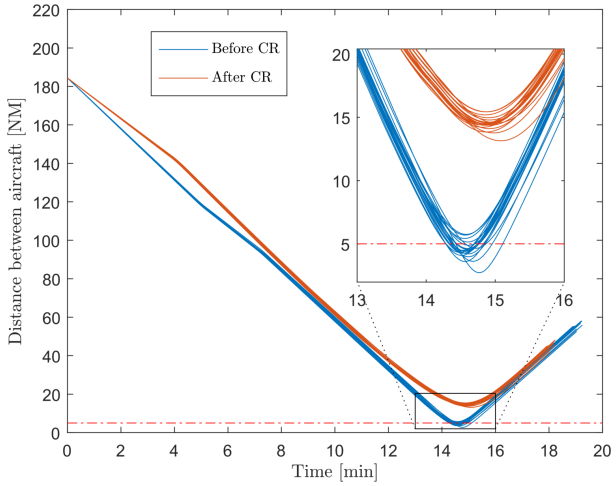

Figure 10. Distance between two aircraft over time for each ensemble member.

The nominal paths of the low-density-scenario flights are depicted in Figure 11(a). In total, 11 high-probability conflicts (with probability $P_{con} \geq 50\%$) are detected; their locations are represented by red marks. Five of these conflicts correspond to losses of separation at the starting time (as given by the filed flight plans); therefore, they are tactical conflicts not solved by the CR method here presented. Additionally, another 4 low-probability conflicts ($P_{con} < 50\%$) are detected. The nominal value of the cost function is $\Phi_0 = 9.9$.

The resolution paths, obtained after the application of the CDR methodology developed in this paper, are shown in Figure 11(b); results are summarized in Table I. The number of high-probability conflicts is reduced, from 11 to 5 (the remaining unresolved conflict correspond to losses of separation at the starting time, which cannot be solved), and the number of low-intensity conflicts is reduced from 2 to zero. The value of the cost function is reduced to $\Phi_{best} = 4.5 \cdot 10^{-4}$.

The nominal paths of the high-density-scenario flights are depicted in Figure 12(a). In this scenario, 88 high-probability conflicts are initially detected, 8 times more than in the low-density scenario. Some hotspots can be observed, where many conflicts take place, e.g. at the South-West and the North-West. The number of low-probability conflicts is 12, and the nominal value of the cost function is $\Phi_0 = 146.5$. The resolution paths are shown in Figure 12(b). The number of high-probability conflicts is reduced to 14: 13 of them correspond to losses of separation at the starting time, which are disregarded; the other remaining conflict corresponds to a face-to-face severe encounter that the CDR algorithm is not able to resolve because the aircraft are already very close at the start, it should be solved tactically. The number of low-intensity conflicts increases from 12 to 20. These low-intensity conflicts may not realise or, if their probabilities increase along time, may be solved in posterior executions of the CDR algorithm. The value of the cost function is reduced to $\Phi_{best} = 4.2$.

TABLE I. CDR results for P_τ = 50%.

Scenario		Number of conflicts: Low prob.	Number of conflicts: High prob.	Φ
Low density ($N = 92$)	Nominal	2	11	9.9
	After CDR	0	5	$4.5{\cdot}10^{-4}$
High density ($N = 214$)	Nominal	12	88	146.5
	After CDR	20	14	4.2

VII. Conclusions

In this work, a probabilistic methodology for strategic conflict detection and resolution, up to 60 minutes in advance, for en-route aircraft under wind and temperature uncertainties has been introduced. The resolution trajectories are generated by modifying the route waypoints (vectoring), with the aim of lowering the probabilities of the conflicts below a given threshold; the probabilistic analysis has been based on an ensemble approach, where the weather uncertainty is retrieved from Ensemble Prediction Systems.

The methodology has been successfully applied to two different en-route conflict scenarios, with very different traffic densities and with hundreds of aircraft. The numerical results show that the number of high-probability conflicts, even in the very demanding artificial scenario, can be significantly reduced. The aim of this methodology is to expand the time horizons of conflict detection and resolution tools currently in use in Europe, enabling the planning of more efficient trajectories and reducing the workload of air traffic controllers.

This work constitutes a first step on the development of a fully functional methodology, that will consider all phases of the flight and will cover an extended geographical area. The development of this complete methodology will involve the extension of the work to the three-dimensional case, and the consideration and integration of different global and regional Ensemble Prediction Systems to widen the coverage area. Additional sources of uncertainty, such as the aircraft departure times, will also be included. Next steps in this line of research will also allow for new decision variables, such as the aircraft speeds or flight levels.

Acknowledgments

The authors gratefully acknowledge the financial support of the Spanish Ministerio de Ciencia, Innovación y Universidades through Grant RTI2018-098471-B-C31.

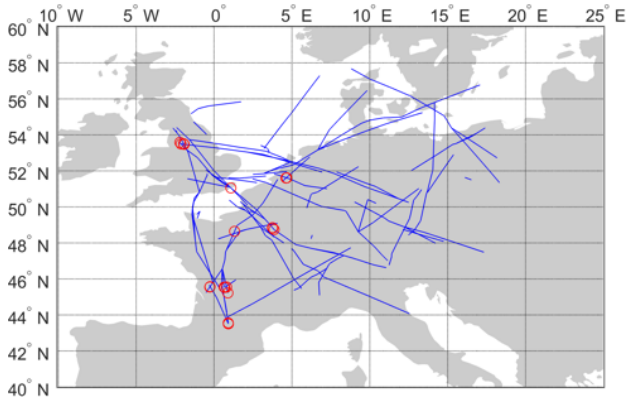

(a) Nominal paths.

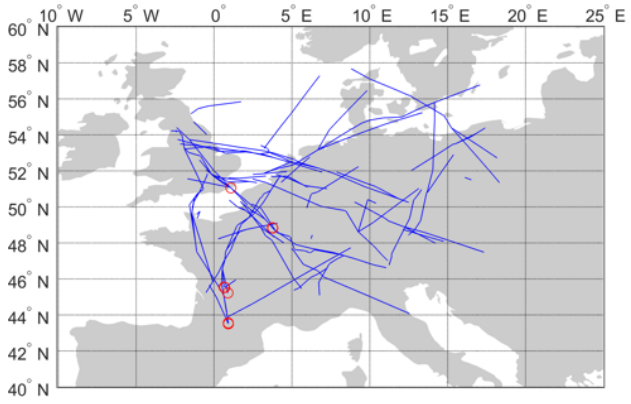

(b) Resolution paths.

Figure 11. Low-density scenario.

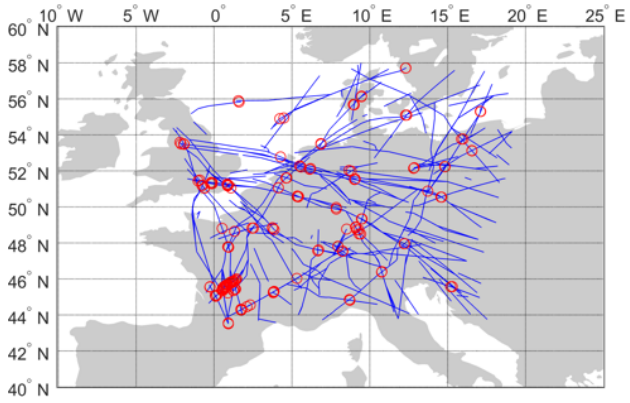

(a) Nominal paths.

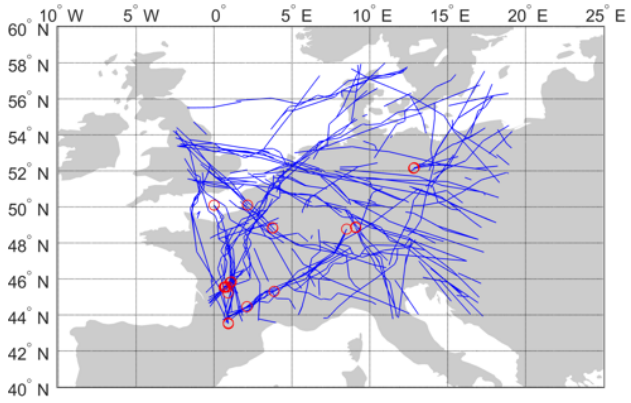

(b) Resolution paths.

Figure 12. High-density scenario.

REFERENCES

[1] D. Rivas and R. Vazquez, "Uncertainty," in Complexity Science in Air Traffic Management, A. Cook and D. Rivas Ed., Ashgate Publishing Limited, 2016, Chap. 4.

[2] International Civil Aviation Organization, "Doc. 9750. Global Air Navigation Plan," Third Edition, 2007, pp. 1–23.

[3] J. K. Kuchar and L. C. Yang, "A review of conflict detection and resolution modeling methods," *IEEE Transactions on Intelligent Transportation Systems*, Vol. 1, No. 4, 2000, pp. 179–189.

[4] Y. Matsuno, T. Tsuchiya, J. Wei, I. Hwang, and N. Matayoshi, "Stochastic optimal control for aircraft conflict resolution under wind uncertainty," *Aerospace Science and Technology*, Vol. 43, 2015, pp. 77–88.

[5] O. Rodionova, B. Sridhar, and H. K. Ng, "Conflict resolution for wind-optimal aircraft trajectories in North Atlantic oceanic airspace with wind uncertainties," Proceedings on the 2016 IEEE/AIAA 35th Digital Avionics Systems Conference (DASC), Sep., 2016, pp. 1–10.

[6] M. Steiner, R. Bateman, D. Megenhardt, Y. Liu, M. Pocernich, and J.A. Krozel, "Translation of ensemble weather forecasts into probabilistic air traffic capacity impact," *Air Traffic Control Quarterly*, Vol. 18, 2010, pp. 229–254.

[7] A. Franco, D. Rivas, and A. Valenzuela, "Probabilistic aircraft trajectory prediction in cruise flight considering ensemble wind forecasts," *Aerospace Science and Technology*, Vol. 82–83, 2018, pp. 350–362.

[8] E. Hernández-Romero, A. Valenzuela, and D. Rivas, "Probabilistic aircraft conflict detection and resolution considering wind uncertainty," Proc. 7th SESAR Innovation Days (SID), pp. 1–8, 2017.

[9] E. Hernández-Romero, A. Valenzuela, and D. Rivas, "A probabilistic approach to measure aircraft conflict severity considering wind forecast uncertainty," *Aerospace Science and Technology*, Vol. 86, 2019, pp. 401–414.

[10] V. Courchelle, M. Soler, D. Gonzlez-Arribas, and D. Delahaye, "A simulated annealing approach to 3D strategic aircraft deconfliction based on en-route speed changes under wind and temperature uncertainties," *Transportation Research Part C: Emerging Technologies*, Vol. 103, 2019, pp. 194–210.

[11] S. Chaimatanan"Planification stratégique de trajectoires d'avions," PhD Thesis. Universit Toulouse III-Paul Sabatier, 2014.

[12] World Meteorological Organization, "Guidelines on Ensemble Prediction Systems and Forecasting," WMO-No. 1091, 2012.

[13] M. Baldauf, C. Gebhardt, S. Theis, B. Ritter, and C. Schraff, "Beschreibung des operationellen Kürzestfristvorhersagemodells COSMO-D2 und COSMO-D2-EPS und seiner Ausgabe in die Datenbanken des DWD," Deutscher Wetterdienst (DWD), Offenbach, Germany, 2018.

[14] Deutscher Wetterdienst, "NWP forecast data," https://www.dwd.de/EN/ourservices/nwp_forecast_data/nwp_forecast_data.html, accessed: 2019-04.

[15] M. Jardin, "Grid-based strategic air traffic conflict detection," *AIAA Guidance, Navigation, and Control Conference and Exhibit*, San Francisco, California, 2019, pp. 1–11.

[16] E. J. Hastings, J. Mesit, and R. K. Guha, "Optimization of large-scale, real-time simulations by spatial hashing," Proc. 2005 Summer Computer Simulation Conference, 2005, Vol. 37, No. 4, pp. 9–17.

[17] International Civil Aviation Organization, "Aircraft Operations. Volume II: Construction of Visual and Instrument Flight Procedures", ICAO, Montréal, Canada, 5ed, 2006.

[18] S. Kirkpatrick, C. D. Gelatt, and M. P. Vecchi, "Optimization by simulated annealing," Science, Vol. 220, No. 4598, 1983, pp. 671–680.